PHYSICAL REVIEW E **66**, 041202 (2002)

Surface instability of icicles

Naohisa Ogawa* and Yoshinori Furukawa†
Institute of Low Temperature Sciences, Hokkaido University, Sapporo 060-0819, Japan
(Received 23 October 2001; revised manuscript received 22 April 2002; published 4 October 2002)

Quantitatively unexplained stationary waves or ridges often encircle icicles. Such waves form when roughly 0.1-mm-thick layers of water flow down an icicle. These waves typically have a wavelength of about 1 cm, which is independent of external temperature, icicle thickness, and the volumetric rate of water flow. In this paper, we show that these waves cannot be obtained by a naive Mullins-Sekerka instability but are caused by a quite different type of surface instability related to thermal diffusion and the hydrodynamic effect of a thin water flow.

DOI: 10.1103/PhysRevE.66.041202 PACS number(s): 47.20.Hw, 81.30.Fb

I. INTRODUCTION

Interesting wave patterns often form on growing icicles that are covered with a thin layer of flowing water (see Fig. 1) [1]. For many of these patterns, the wavelength has a Gaussian distribution centered at ≈ 8 mm; however, despite their common occurrence, there is no quantitative explanation for this wavelength distribution [1,2]. These waves are associated with the growth of the icicles and flow of fluid along the icicle. Hence, there are several processes occurring that should be considered. These include crystallization from the melt, latent heating at the ice-melt interface, laminar flow with two interfaces (ice-melt and melt-air), evaporation of liquid, and transport of heat through the surrounding air. The fact that waves tend to encircle the icicle clearly indicates the importance of gravity-induced flow, although the specific interactions between flow, ice growth, and heat flow through both interfaces must be considered.

In studies on crystal growth, such a surface instability is usually explained by the Mullins-Sekerka (MS) theory. The MS theory is based on two observations: Laplace instability and the Gibbs-Thomson (GT) effect. (For detailed explanation, refer to textbooks and the original paper by Mullins and Sekerka cited in Ref. [3].)

To a good approximation, the ice in an icicle has a uniform temperature of 273 K; thus, temperature gradients into the ice are insignificant, and the external temperature field is time independent and satisfies Laplace's equation. We further assume that the external temperature is below 273 K, i.e., the ice is not melting on average. At a convex point, the temperature gradient is higher. Because the heat flow is proportional to the gradient of temperature, the larger heat flow at a convex point rapidly removes latent heat from the ice surface, thus allowing the convex points to increase in size rapidly. Conversely, concave regions grow relatively slowly. This phenomenon suggests that short-wavelength fluctuations increase in amplitude more rapidly than do long wavelength fluctuations. We refer to this as the Laplace instability.

Next, we explain the GT effect. The surface of a solid object has its own energy per area called surface free energy. If a molecule attaches itself to the surface near a convex point, the surface area increases, resulting in an increase in energy. On the other hand, if a molecule becomes attached to the surface near a concave point, absorption of the molecule makes the surface area smaller. Therefore, absorption of a molecule at a concave point is more energy efficient than is absorption at a convex point. For this reason, the melting point depends on the curvature of an object, i.e., the shape of the surface area. The melting point is lower at a convex surface (easy to melt) and is higher at a concave surface (hard to melt). Such an effect suppresses the fluctuation and makes the surface flat. This is called the GT effect, which is opposite to that of the Laplace instability. The Laplace instability enhances shorter wavelength fluctuation, and the GT effect suppresses shorter wavelength fluctuation. From these two effects, we have fluctuation of specific wavelength mainly. These two effects are incorporated in Mullins-Sekerka's theory [3,4]. However, a simple application of this theory is not possible in the case of icicles for the following reasons. First, the water layers on icicles are too thin to cause Laplace instability, because the instability requires that the

FIG. 1. Waves on icicles.

*Email address: ogawa@particle.sci.hokudai.ac.jp
†Email address: frkw@lowtem.hokudai.ac.jp

 ©2002 The American Physical Society

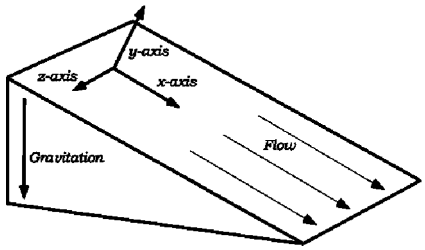

FIG. 2. Flow on a ramp inclined at θ deg.

water thickness be larger than the wavelength of the fluctuation. Second, the curvature is too small. (Wavelength of 1 cm is much larger than 10 μm, which is required for the GT effect.) Therefore, the nature of wave patterns along icicles cannot be explained by the naive MS theory.

We neglect the fluid instabilities that require turbulence because there should be no turbulence in these water films [6]. This is because the layers are only about 100 μm thick and the flow speeds are about 2–4 cm/s; the resulting Reynolds numbers are only about 1 and the flow is laminar. The hydrodynamics of a thin water layer is also discussed by Wettlaufer *et al.* to explain the premelting dynamics, but the discussion here is essentially different [5].

For our analysis, we assume water flow on a ramp (see Fig. 2.) because it is simpler to treat and results of relevant experiments for this geometry have been reported [2]. Much of the same processes and relative length scales occur in both systems because the water-layer thickness ($\sim 10^{-4}$m) is much smaller than the radius of the icicle ($\sim 10^{-2}$m). Furthermore, Matsuda [2] observed wave patterns on such an ice ramp; for example, at $\theta = \pi/2$, the wavelength was about 8 mm.

Liquid flow of a thin water layer on a flat ramp (Benney's liquid film) produces waves [7] (see also Ref. [8]); however, these waves travel down the ramp and are thus unlike the case on icicles. Due to the explicit calculation, the wavelength of these traveling surface waves is about 1 cm, similar to the wavelength along icicles, but they move at about 4–8 cm/s, which is twice the speed of the fluid. Benney's wave is caused by gravity and surface tension, but it is unclear how it applies to the standing waves on ice unless the traveling waves can become pinned to a fixed location; such a pinning mechanism has not yet been proposed.

Our approach is to assume static flow with small ripples on the ramp surface and then calculate the growth rate for the ripples by solving the thermal diffusion equation in the background fluid. In Sec. II, we discuss the fluid dynamics of a thin layer of water flowing along a ramp, and then in Sec. III, we couple the thermal diffusion process to the flow. The thermal diffusion in air is solved in Sec. IV. In Sec. V, we discuss the growth rate of fluctuation on icicles by combining the solutions for thermal diffusion equations in two regions: air and water.

II. HYDRODYNAMICS OF A THIN LAYER OF WATER

We consider the fluid mechanics of a thin water layer with depth $h(x)$ as sketched in Fig. 3. Over each wavelength, the average depth is h_0. There are two material boundaries: the solid-liquid boundary (SL) and the air-liquid boundary (AL). The x axis is along the ramp and increases in the downhill direction, whereas the y axis is the outward normal to the ramp. The SL surface is not flat and is given by

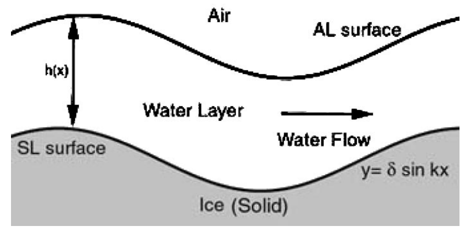

FIG. 3. Two boundaries: SL and AL.

$$y = \phi(x), \qquad \phi(x) = \delta \sin kx. \tag{1}$$

The AL surface is given by

$$y = \xi(x) \equiv \phi(x) + h(x) \qquad \text{with} \qquad \langle h(x) \rangle = h_0, \tag{2}$$

where $\langle h \rangle$ means average over the wavelength in the x axis direction.

The results of a previous experimental study [2] showed that the surface velocity of the fluid is about 3 cm/s, and by using the Nusselt equation, which is shown later [8], the average water-layer thickness h_0 was calculated to be around 0.1 mm. The wavelength $\lambda = 2\pi/k$ was experimentally determined to be about 1 cm. We use the parameter

$$\mu \equiv kh_0, \tag{3}$$

which is 6×10^{-2}, for the typical experimental values above. In general, $\mu \ll 1$ defines the long-wavelength approximation.

Our key assumptions are as follows: (1) steady-state (time-independent) flow, (2) $\mu \ll 1$ (long-wavelength approximation), and (3) incompressible fluid.

We prefer to use the following dimensionless variables. For length,

$$x \to x_* \equiv kx, \tag{4}$$

$$y \to y_* \equiv y/h_0. \tag{5}$$

The thickness of the water layer is thus

$$h(x) \to h^*(x) = h(x)/h_0 = 1 + \tilde{h}(x), \tag{6}$$

and the respective heights of the SL and AL surfaces are

$$\phi_*(x) = (\delta/h_0)\sin x_* \equiv \eta \sin x_*, \tag{7}$$

$$\xi_*(x) = h_*(x) + \phi_*(x) = 1 + \tilde{h}(x) + \eta \sin x_*. \tag{8}$$

The characteristic flow velocity in the x direction is

$$U_0 = \frac{g h_0^2 \sin\theta}{2\nu}, \tag{9}$$

where g is the gravitational acceleration and the viscosity $\nu = 1.8\times10^{-6}$ m^2/s at 0 °C. This is a Nusselt equation, the theoretically predicted velocity at the AL surface when $\delta = 0$, i.e., for a flat SL surface with uniform thickness [8]. This unperturbative solution is obtained by equating the gravitational force to the viscous force. The velocity distribution is parabolic in y,

$$v_x = U_0\left(2\frac{y}{h_0} - \left[\frac{y}{h_0}\right]^2\right). \tag{10}$$

We consider perturbations of this solution. By using the above formula for speed, we relate the experimentally determined flow Q to h_0 and surface velocity U_0. The flow quantity is defined by $Q = 2\pi R\overline{U}h_0$, where $\overline{U} = 1/h_0\int_0^{h_0} v_x dy = 2U_0/3$, the mean speed, and R is the radius of the icicle. In an experiment [2], Matsuda used the flow $Q = 160$ ml/hr and width of gutter $l = 3$ cm (l corresponds to $2\pi R$) because this produced the clearest waves. This gives $\overline{U}h_0 = 1.48\times10^{-6}$ m^2/s. From $\overline{U} = 2U_0/3$ and $U_0 = gh_0^2/2\nu$ (by setting $\theta = \pi/2$), we get $U_0 = 2.4\times10^{-2}$ m/s with $h_0 = 0.93\times10^{-4}$ m. On the other hand, his measurement of the surface mean velocity by observing the motion of fine grain was $U_0 = 4\times10^{-2}$ m/s at $\theta = \pi/2$. Hence, we assume $U_0 = (2.4\sim4)\times10^{-2}$ m/s with $h_0 = (0.93\sim1.21)\times10^{-4}$ m as the experimental surface speed and water-layer thickness.

In the y direction, characteristic velocity is

$$V_0 = \mu U_0. \tag{11}$$

We denote speed in the x direction as u, that in the y direction as v, and pressure as P. Dimensionless speeds and pressure are given by

$$u_* = u/U_0, \tag{12}$$

$$v_* = v/V_0, \tag{13}$$

$$P_* = \frac{P}{\rho g h_0 \sin\theta}. \tag{14}$$

Other dimensionless constant parameters are the Reynolds number Re and the Weber number W.

$$\mathrm{Re} \equiv \frac{h_0 U_0}{\nu}, \tag{15}$$

$$W \equiv \frac{\gamma}{\rho g h_0^2}, \tag{16}$$

where $\gamma \sim 7.6\times10^{-2}$ N/m is the surface tension of liquid water. Approximate values of these quantities, $U_0 \sim 3\times10^{-2}$ m/s, $h_0 \sim 10^{-4}$ m, and $\nu \sim 1.8\times10^{-6}$ m^2/s predict $\mathrm{Re} \sim 1.5$ and $W \sim 10^3$. This value of the Reynolds number indicates a laminar flow. The flow components u and v satisfy the steady-state Navier-Stokes equation for incompressible fluids,

$$(\mathbf{v}\cdot\boldsymbol{\nabla})\mathbf{v} = -\frac{\boldsymbol{\nabla}P}{\rho} + \mathbf{g} + \nu\Delta\mathbf{v}. \tag{17}$$

The incompressibility condition is

$$\boldsymbol{\nabla}\cdot\mathbf{v} = \mathbf{0}. \tag{18}$$

The mass conservation law at the water-air interface requires

$$\frac{d\xi}{dx} = \frac{v(x,\xi(x))}{u(x,\xi(x))}. \tag{19}$$

The boundary conditions at the SL surface are zero fluid velocity,

$$u(x,y=\phi(x)) = 0, \qquad v(x,y=\phi(x)) = 0. \tag{20}$$

The stress balancing condition on AL surface, that is, the free surface condition is

$$P_{(In)}n_i = \hat{P}n_i + \rho\nu\left(\frac{\partial v_i}{\partial x^k} + \frac{\partial v_k}{\partial x^i}\right)n_k - \gamma\frac{d^2\xi(x)}{dx^2}n_i. \tag{21}$$

The index means $x^1 = x$ and $x^2 = y$, and n_i is the normal unit vector to the AL surface. $P_{(In)}$ is the pressure just under the AL surface, and $\hat{P}$ is the atmospheric pressure. For the above equations, we approximated the surface tension term as $\gamma\xi''$ by neglecting the second-order term in μ.

Now we rewrite the equations in dimensionless form. The incompressible fluid condition is

$$\frac{\partial u_*}{\partial x_*} + \frac{\partial v_*}{\partial y_*} = 0.$$

For this condition to hold automatically, we introduce the dimensionless stream function by

$$u_* = \frac{\partial\psi}{\partial y_*}, \qquad v_* = -\frac{\partial\psi}{\partial x_*}. \tag{22}$$

In the following, we use the stream function instead of velocity. Also, we drop the * mark on the dimensionless quantities. All of the quantities in the remainder of this section are dimensionless.

Now the Navier-Stokes equation becomes

$$\psi_{yyyy} = \mu\,\mathrm{Re}[\psi_y\psi_{xyy} - \psi_x\psi_{yyy}] - 2\mu^2\psi_{xxyy} - \mu^3\,\mathrm{Re}[\psi_x\psi_{xxy} - \psi_y\psi_{xxx}] - \mu^4\psi_{xxxx}, \tag{23}$$

where the indices indicate derivatives with respect to x and y. The fourth-order derivatives appearing on the left-hand side come from the viscous term by taking the derivative to cancel the pressure term in Eq. (17). The pressure is determined from the Navier-Stokes equation by using the stream function as follows:

$$P_x = \frac{1}{\mu} + \frac{1}{2\mu}\psi_{yyy} - \frac{\mathrm{Re}}{2}(\psi_y\psi_{xy} - \psi_x\psi_{yy}) + \frac{\mu}{2}\psi_{xxy}, \tag{24}$$

or

$$P_y=-\cot\theta-\frac{\mu}{2}\psi_{xyy}-\frac{\mu^3}{2}\psi_{xxx}-\frac{\mu^2\,\mathrm{Re}}{2}(-\psi_y\psi_{xx}+\psi_x\psi_{xy}). \tag{25}$$

For the stream function, we include only the zeroth and first-orders in μ, and for pressure, only the zeroth-order terms are kept.

The Navier-Stokes equation for the stream function and the pressure equations become

$$\psi_{yyyy}=\mu\,\mathrm{Re}[\psi_y\psi_{xyy}-\psi_x\psi_{yyy}], \tag{26}$$

$$P_x=\frac{1}{\mu}+\frac{1}{2\mu}\psi_{yyy}-\frac{\mathrm{Re}}{2}(\psi_y\psi_{xy}-\psi_x\psi_{yy}), \tag{27}$$

$$P_y=-\cot\theta. \tag{28}$$

Next we consider the boundary conditions up to $O(\mu)$.

$$\psi_x(x,y=\phi)=\psi_y(x,y=\phi)=0, \tag{29}$$

$$P(x,y=\xi)=\hat{P}-\frac{W_0}{\sin\theta}(\tilde{h}_{xx}-\eta\sin x)-\mu\psi_{xy}, \tag{30}$$

$$\psi_{yy}(x,y=\xi)=0, \tag{31}$$

$$\tilde{h}_x+\eta\cos x=-\frac{\psi_x}{\psi_y}(x,y=\xi), \tag{32}$$

where we define $W_0\equiv\mu^2W\sim10^0$ as order one, because W is 7.6×10^2 in our case.

When $\eta=\tilde{h}=0$, a flat laminar flow occurs with the solution

$$\psi=-\tfrac{1}{3}y^3+y^2,\qquad P=\hat{P}+(1-y)\cot\theta, \tag{33}$$

which is easily shown to satisfy the Navier-Stokes equation and all boundary conditions.

Therefore, we consider the perturbations from this solution. The precise perturbative calculations are given in the Appendix, and as a result, we obtain the height of the AL surface,

$$\xi(x)=1+\eta\sin x, \tag{34}$$

and the stream function given by

$$\psi=-\tfrac{1}{3}(y-\eta\sin x)^3+(y-\eta\sin x)^2. \tag{35}$$

In our approximation, we have only the zeroth-order terms in μ. This is because the first-order terms in μ are also proportional to the small quantity η, the amplitude of a small ripple, which makes them effectively second-order quantities. The form of the stream function is intuitively understood easily, because it is just a modification of the unperturbative solution for the velocity to vanish at a nonflat SL boundary.

III. THERMAL DIFFUSION PROCESS IN THE WATER LAYER

A. Basic equation

Now we consider the thermal diffusion process in the fluid that was obtained in the preceding section. We make the following assumptions: (1) long-wavelength approximation is used up to the first order in μ ($\mu\equiv kh_0\sim6\times10^{-2}$); (2) thermal expansion of the water is ignored, and incompressible fluid is thus retained; and (3) heat transport is through steady-state thermal diffusion with flow.

Note that the steady state is valid because the time scale for temperature change is much longer than the time scale for ice crystal growth. The heat flow is given by $\vec{Q}\equiv-\kappa\vec{\nabla}T+(\rho cT)\vec{v}$, where κ is the thermal conductivity of water, T is the temperature, and c is the specific heat of water. The steady-state continuity condition is given by dropping the time derivative,

$$\triangle T-\frac{\vec{v}}{D}\cdot\vec{\nabla}T=0, \tag{36}$$

where $D\equiv\kappa/\rho c$ is the thermal diffusivity of water, and the incompressibility condition was used. Furthermore, we dropped the term for the thermal energy coming from energy dissipation of fluid [8],

$$-\frac{\rho\nu}{2\kappa}\left(\frac{\partial v_i}{\partial x_k}+\frac{\partial v_k}{\partial x_i}\right)^2, \tag{37}$$

because this term is much smaller than the other terms. Below we use dimensionless parameters (x_*,y_*) again. From the preceding section,

$$u=U_0\frac{\partial\psi}{\partial y_*},\qquad v=-\mu U_0\frac{\partial\psi}{\partial x_*},$$

where ψ is the dimensionless stream function. Equation (36) becomes

$$\frac{\partial^2T}{\partial y_*^2}=\alpha\left[\frac{\partial\psi}{\partial y_*}\frac{\partial T}{\partial x_*}-\frac{\partial\psi}{\partial x_*}\frac{\partial T}{\partial y_*}\right], \tag{38}$$

where we have dropped the μ^2 term. From experimental results, $D\sim1.3\times10^{-7}$, $\mu\sim6\times10^{-2}$, $U_0\sim3\times10^{-2}$, and $h_0\sim10^{-4}$. This gives

$$\alpha\equiv\mu\frac{h_0U_0}{D}\sim1.4.$$

In the following sections, we drop the * mark on the dimensionless quantities again.

B. Expansion in powers of y

We start from Eq. (38) with the stream function (35). The temperature at the SL boundary will be nearly equal to the melting temperature $T_M=273.15$ K at atmospheric pressure. The surface tension for the curvatures in the experiment

(Gibbs-Thomson effect) can alter the melting temperature by at most 10^{-6} K, which can be neglected. Hence, we expand the solution in powers of $Y \equiv y - \eta \sin x$.

$$T(x,y) = T_M + a_1(x)Y + a_2(x)Y^2 + \cdots . \tag{39}$$

The left and right sides of Eq. (38) become

$$T_{yy} = T_{YY} = \sum_{k=2}^{\infty} k(k-1)a_k(x)Y^{k-2}, \tag{40}$$

$$\frac{\partial\psi}{\partial y}\frac{\partial T}{\partial x} - \frac{\partial\psi}{\partial x}\frac{\partial T}{\partial y} = \frac{\partial\psi}{\partial Y}\frac{\partial T}{\partial x}\bigg|_Y - \frac{\partial\psi}{\partial x}\bigg|_Y \frac{\partial T}{\partial Y}$$
$$= (2Y - Y^2)\sum_{k=1}^{\infty}\frac{da_k(x)}{dx}Y^k. \tag{41}$$

Making the left and right sides of Eq. (38) equal gives

$$\sum_{k=2}^{\infty} k(k-1)a_k(x)Y^{k-2} = \alpha Y(2-Y)\sum_{k=1}^{\infty}\frac{da_k(x)}{dx}Y^k. \tag{42}$$

The coefficients are found recursively,

$$a_{n+4} = \frac{\alpha}{(n+4)(n+3)}\frac{d}{dx}\{2a_{n+1} - a_n\},$$
$$a_2 = a_3 = 0, \qquad a_4 = \frac{\alpha}{6}\frac{da_1(x)}{dx}. \tag{43}$$

All of the coefficients are determined when $a_1(x) \equiv a(x)$ is known. The first nine coefficients are as follows by using the definition $\hat{D} \equiv \alpha d/dx$:

$$a_1 = a,$$
$$a_2 = 0,$$
$$a_3 = 0,$$
$$a_4 = \frac{\hat{D}}{6}a,$$
$$a_5 = -\frac{\hat{D}}{20}a,$$
$$a_6 = 0,$$
$$a_7 = \frac{\hat{D}^2}{126}a,$$
$$a_8 = -\frac{\hat{D}^2}{210}a,$$
$$a_9 = \frac{\hat{D}^2}{1440}a.$$
$$\cdots$$

Because $\alpha \sim O(1)$, we consider only these second-derivative terms.

On the SL surface,

$$T(SL) = T_M = \text{const} \tag{44}$$

$$\mathcal{Q}(SL) = -\kappa \frac{\partial T}{\partial y}\bigg|_{y=\eta \sin x} = -\kappa a(x). \tag{45}$$

On the AL surface,

$$T(AL) = T_M + \left[1 + \frac{7}{60}\hat{D} + \frac{13}{3360}\hat{D}^2\right]a(x), \tag{46}$$

$$\mathcal{Q}(AL) = -\kappa\left[1 + \frac{5}{12}\hat{D} + \frac{239}{10\,080}\hat{D}^2\right]a(x), \tag{47}$$

where $\mathcal{Q}$ is the heating resulting from the temperature gradients. We have omitted the $O(\hat{D}^3)$ terms. The additional terms are $(6.0\times10^{-5})\hat{D}^3 a$ in Eq. (46) and $-\kappa(5.2\times10^{-4})\hat{D}^3 a$ in Eq. (47). To be comparable with the $O(\hat{D}^2)$ term, α needs to be about 10^2. Therefore, this approximation is valid when $\alpha \ll 10^2$. To determine $a(x)$, we must consider the temperature and heat flow at the AL surface.

IV. THERMAL DIFFUSION IN AIR

We consider the thermal diffusion in air to consider the temperature and heat flow at the AL surface. We note two points here. First, we cannot approximate the icicle system as a ramp. The ramp picture is a good approximation when we consider the inside of the thin water layer but not good for the outside. Therefore, we treat the icicle as a cylindrical object and consider the thermal diffusion outside. Second, we cannot use the same dimensionless variable as before since our physical space is the outside. Therefore, we use different-dimensional coordinates in this section. The diffusion equation in air is given by

$$\Delta T = 0. \tag{48}$$

Let us write down in cylindrical coordinate,

$$\left[\frac{\partial^2}{\partial r^2} + \frac{1}{r}\frac{\partial}{\partial r} + \frac{1}{r^2}\frac{\partial^2}{\partial\theta^2} + \frac{\partial^2}{\partial x^2}\right]T(r,\theta,x) = 0. \tag{49}$$

We assume axial symmetry, and so we have $\partial T/\partial\theta = 0$. Therefore, we work with

$$\left[\frac{\partial^2}{\partial r^2} + \frac{1}{r}\frac{\partial}{\partial r} + \frac{\partial^2}{\partial x^2}\right]T(r,x) = 0. \tag{50}$$

Because the surface oscillates in the x direction, we assume that the solution has the form

$$T(r,x) = f(r) + g(r)\sin(kx + \phi), \tag{51}$$

where we have assumed that the icicle is an infinitely long column with small surface fluctuations. $f(r)$ satisfies

$$\left[\frac{d^2}{dr^2}+\frac{1}{r}\frac{d}{dr}\right]f(r)=0, \tag{52}$$

and $g(r)$ satisfies

$$\left[\frac{d^2}{dr^2}+\frac{1}{r}\frac{d}{dr}-k^2\right]g(r)=0. \tag{53}$$

The solution is

$$T(r,x)=A+B\ln(r/R)+CK_0(kr)\sin(kx+\phi), \tag{54}$$

where K_0 is the zeroth-modified Bessel function, and A, B, and C are constants. R is the mean radius of the icicle, including the thickness of the water layer h_0. Note that the constant C is of the order δ, because it is introduced from the fluctuation on an icicle. We define the local coordinate y by

$$r=R+y.$$

The solution is

$$T(x,y)=A+B\ln(1+y/R)+CK_0(k(R+y))\sin(kx+\phi). \tag{55}$$

Note that the ramp system is retained by taking the limit $R\to\infty$ with fixing B/R and $C\exp(-kR)$ finite:

$$T(x,y)=A+B'y+C'\exp(-ky)\sin(kx+\phi),$$

where B' and C' are other constants. Hereafter we work with the case of finite R, because the ramp case is always retained by taking the limit as above. The reader might consider the appearance of a logarithmic term to be strange, since it diverges at large r. But the appearance of such a term is natural for an infinitely long axially symmetric source. As real icicles have finite lengths, this solution is valid only close to the icicle; far from the icicle, the icicle acts like a point source of heat and we must match the near-icicle and far-icicle solutions at $r\sim L$, where L is the length of the icicle. This matching includes that of temperature at infinity and partly determines the coefficients A, B, and C; in addition, the mean growth rate of the icicle radius also determines coefficient B, which includes information on the temperature at infinity.

Near the AL surface, $y\ll R$, we have

$$\begin{aligned}T(x,y)&=A+\frac{B}{R}y+\cdots+C[K_0(kR)+K_0'(kR)ky+\cdots]\\&\quad\times\sin(kx+\phi)\sim[A+CK_0(kR)\sin(kx+\phi)]\\&\quad+\left[\frac{B}{R}+CkK_0'(kR)\sin(kx+\phi)\right]y\\&\quad+\frac{1}{2}\left[-\frac{B}{R^2}+Ck^2K_0''(kR)\sin(kx+\phi)\right]y^2+\cdots,\end{aligned} \tag{56}$$

where K' and K'' indicate derivatives of K with respect to its argument. We define the mean growth rate of an icicle V by

$$V\equiv-\frac{\kappa_0}{L}\left\langle\frac{\partial T}{\partial y}\right\rangle_{y=0}=-\frac{\kappa_0 B}{LR}, \tag{57}$$

where κ_0 is the thermal conductivity of air, and $\langle\rangle$ means spatial average over x. So we obtain

$$B=-\frac{LRV}{\kappa_0}. \tag{58}$$

At $y=\delta\sin kx$ (AL surface), the temperature and heat flow are

$$\begin{aligned}T_{AL}&=[A+CK_0(kR)\sin(kx+\phi)]\\&\quad+\left[-\frac{LV}{\kappa_0}+CkK_0'(kR)\sin(kx+\phi)\right]\delta\sin kx\\&=A+\left[CK_0(kR)\cos\phi-\frac{LV}{\kappa_0}\delta\right]\sin kx\\&\quad+CK_0(kR)\sin\phi\cos kx,\end{aligned} \tag{59}$$

$$\begin{aligned}\mathcal{Q}_{AL}&=LV-\left[\kappa_0 CkK_0'(kR)\cos\phi+\frac{LV\delta}{R}\right]\sin kx\\&\quad-\kappa_0 CkK_0'(kR)\sin\phi\cos kx.\end{aligned} \tag{60}$$

Because the constant C is of the order δ, we have dropped δC terms, and we keep terms up to the first order in δ.

V. GROWTH RATE

Two boundary conditions apply to the AL surface: continuous temperature and continuous heat flow across the water-air boundary. Comparing these two sets of equations, Eqs. (46) and (59) and Eqs. (47) and (60), the solution requires that $a(x)=E+F\sin kx+G\cos kx$, where E,F, and G are constants with dimension of temperature.

Then, in-dimensional units, Eqs. (46) and (47) are

$$\begin{aligned}T_{AL}&=T_M+E+\left[F-\frac{7\alpha}{60}G-\frac{13\alpha^2}{3360}F\right]\sin kx\\&\quad+\left[G+\frac{7\alpha}{60}F-\frac{13\alpha^2}{3360}G\right]\cos kx,\end{aligned} \tag{61}$$

$$\begin{aligned}\mathcal{Q}_{AL}&=-\frac{\kappa}{h_0}E-\frac{\kappa}{h_0}\left[F-\frac{5\alpha}{12}G-\frac{239\alpha^2}{10\,080}F\right]\sin kx\\&\quad-\frac{\kappa}{h_0}\left[G+\frac{5\alpha}{12}F-\frac{239\alpha^2}{10\,080}G\right]\cos kx.\end{aligned} \tag{62}$$

By comparing with Eqs. (59) and (60), we have six equations with six unknowns (i.e., A, C, ϕ, E, F, and G). A and E can be calculated beforehand,

$$A = T_M - \frac{LVh_0}{\kappa}, \tag{63}$$

$$E = -\frac{LVh_0}{\kappa}. \tag{64}$$

The other four quantities are determined by the following equations:

$$\begin{pmatrix} 1-\frac{13\alpha^2}{3360} & -\frac{7\alpha}{60} \\ \frac{7\alpha}{60} & 1-\frac{13\alpha^2}{3360} \end{pmatrix} \begin{pmatrix} F \\ G \end{pmatrix} = \begin{pmatrix} CK_0(kR)\cos\phi - \frac{LV\delta}{\kappa_0} \\ CK_0(kR)\sin\phi \end{pmatrix}, \tag{65}$$

$$\begin{pmatrix} 1-\frac{239\alpha^2}{10\,080} & -\frac{5\alpha}{12} \\ \frac{5\alpha}{12} & 1-\frac{239\alpha^2}{10\,080} \end{pmatrix} \begin{pmatrix} F \\ G \end{pmatrix} = \begin{pmatrix} \frac{\kappa_0}{\kappa}\mu K_0'(kR) C\cos\phi + \frac{LVh_0\delta}{R\kappa} \\ \frac{\kappa_0}{\kappa}\mu K_0'(kR) C\sin\phi \end{pmatrix}. \tag{66}$$

Solving the above equations, we obtain

$$F = \mu \frac{LV\delta K_0'}{\kappa K_0} \frac{1-\frac{239}{10\,080}\alpha^2}{1+\frac{1272}{10\,080}\alpha^2 + \left(\frac{239}{10\,080}\right)^2\alpha^4}, \tag{67}$$

$$G = -\mu \frac{LV\delta K_0'}{\kappa K_0} \frac{\frac{5}{12}\alpha}{1+\frac{1272}{10\,080}\alpha^2 + \left(\frac{239}{10\,080}\right)^2\alpha^4}, \tag{68}$$

where we have neglected second-order terms in μ and we have neglected a term proportional to $h_0/R(\sim 10^{-3})$.

At the SL surface, the growth rate of ice is given by

$$v(x) = \frac{Q_{SL}}{L} = V - \frac{\kappa}{Lh_0}(F\sin kx + G\cos kx). \tag{69}$$

The form of the growth rate is different from that in the usual MS theory. In the MS theory, $v(x) = V + f\sin kx$ for the surface $y = \delta \sin kx$. But now we have another term, $\cos kx$. To understand its physical meaning, we write the relative growth rate v_s as the growth rate in a reference frame moving with velocity V $(v_s \equiv v - V)$.

$$v_s(x) = f\sin kx - g\cos kx, \tag{70}$$

$$f \equiv -\frac{\kappa}{Lh_0}F, \qquad g \equiv \frac{\kappa}{Lh_0}G. \tag{71}$$

The steady-state condition means

$$v_s(x) \equiv \left.\frac{dy_s(x,t)}{dt}\right|_{t=0},$$

where y_s is the height of the SL surface in the reference frame. From the steady-state condition, the time scale for the growth of the fluctuation is very long compared to our observing time scale. By solving the equation

$$v_s(x) \equiv \left.\frac{dy_s(x,t)}{dt}\right|_{t=0} = f\sin kx - g\cos kx \tag{72}$$

with

$$y_s(x, t=0) = \delta \sin kx, \tag{73}$$

we obtain

$$y_s(x,t) = \delta(t)\sin(kx - \omega t) \tag{74}$$

with relations

$$\dot{\delta} = f, \qquad \omega = g/\delta. \tag{75}$$

The essential point is that the fluctuation is not only growing up, but also traveling downwards $(f>0,\ g>0)$. Therefore, the amplification factor is determined from F.

By using the relation $-K_0' = K_1 > 0$, we have

$$\frac{\dot{\delta}}{\delta} = -\frac{\kappa}{Lh_0\delta}F = Vk \frac{\frac{K_1(kR)}{K_0(kR)}\left(1-\frac{239}{10\,080}\alpha^2\right)}{1+\frac{1272}{10\,080}\alpha^2 + \left(\frac{239}{10\,080}\right)^2\alpha^4}. \tag{76}$$

Note that $K_1(kR)/K_0(kR) \sim 1 + 1/2kR$. In the case of $kR \gg 1/2$, meaning a thick icicle, we obtain

$$\frac{\dot{\delta}}{\delta} = Vk \frac{1-\frac{239}{10\,080}\alpha^2}{1+\frac{1272}{10\,080}\alpha^2 + \left(\frac{239}{10\,080}\right)^2\alpha^4}. \tag{77}$$

Because $\alpha \propto k$, this form is similar to that of the amplification factor given by the Mullins-Sekerka theory. The amplification factor increases in proportion to wave number by thermal diffusion in air as expected for a Laplace instability, and it decays by interaction with fluid (α terms). The thermal diffusion in thin water flow works just like the Gibbs-Thomson effect, since the fluid makes the temperature distribution uniform and inhibits the Laplace instability. From these two effects, we obtain the maximum value for $\dot{\delta}/\delta$.

The maximum amplification factor occurs when $\alpha = 2.2$ (Fig. 4), which determines a preferred wavelength,

$$\alpha_{max} \sim 2.2.$$

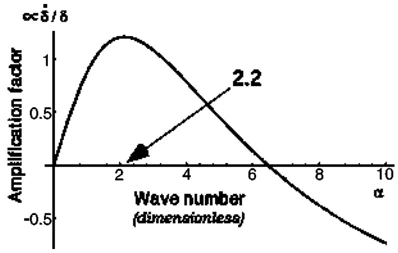

FIG. 4. The dimensionless amplification factor $h_0^2 U\dot{\delta}/DV\delta$ versus the dimensionless wave number α. Laplace instability in air and a GT-like effect due to hydrodynamics amplify perturbations that have a wavelength given by a value of α close to 2.2.

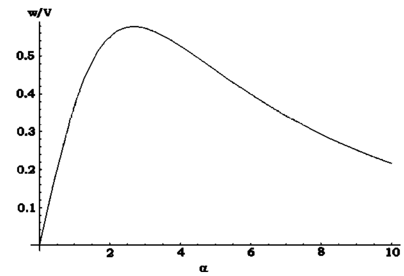

FIG. 5. The dimensionless speed w/V that the ripples travel down an icicle versus $\alpha \sim U_0^2/\lambda$, where V is the growth rate of an icicle.

By using $D=1.3\times10^{-7}$ m^2/s with experimental data,

$$U_0=(2.4\sim4)\times10^{-2}\ \text{m/s},\qquad h_0=(0.93\sim1.21)\times10^{-4}\ \text{m},$$

we have

$$\lambda_{\text{max}}=\frac{2\pi}{k_{max}}=2\pi\frac{h_0^2U_0}{D\alpha_{max}}=5\sim13\ \text{mm},\tag{78}$$

which agrees well with the experimental value of 8 mm [9]. Also, in agreement with observations, this value does not depend directly on external temperature.

Using the constraints between U_0, h_0, and flow quantity Q as

$$U_0=\frac{gh_0^2\sin\theta}{2\nu},\quad Q=\frac{4\pi}{3}RU_0h_0.\tag{79}$$

Then Q is related to λ_{max} as

$$\lambda_{\text{max}}=\frac{1}{D\alpha_{max}}\left(\frac{\nu}{g\pi}\right)^{1/3}\left(\frac{3Q}{2R}\right)^{4/3},$$

where it is assumed that $\theta=\pi/2$. Therefore, if Q is proportional to R for usual icicles, its wavelength is uniquely determined. But for thin icicles with $R\leqslant\lambda/(4\pi)$, we should include the $1/2kR$ term that we have neglected.

Next we consider the travel of fluctuations along the icicle. The traveling phase velocity w is the following function of α:

$$w\equiv\frac{\omega}{k}=\frac{\kappa G}{L\delta h_0k}=\frac{K_1V}{K_0}\beta(\alpha)\sim V\beta(\alpha),\tag{80}$$

where $\beta(\alpha)$ is defined by

$$\beta(\alpha)\equiv\frac{\frac{5}{12}\alpha}{1+\frac{1272}{10\,080}\alpha^2+\left(\frac{239}{10\,080}\right)^2\alpha^4},\tag{81}$$

and its form is given in Fig. 5.

At the 8 mm wavelength, fluctuation travels downwards very slowly with speed $w\sim0.5V$, where V is the mean growth rate ($V=\dot{R}$). For the ambient air temperature of -8 °C, the experimentally determined speed is about 1 mm per hour. Because water flow carries heat flow downwards, this kind of motion seems to be natural. Actually the speed w is zero when $U_0=0$ ($\alpha=0$). Then we can imagine that such speed is an increasing function of fluid velocity U_0. But this is not true. For (solid) surface fluctuation to change its form, it is necessary to emit latent heat nonuniformly. Like the maximization of the amplification (growing) factor at a specific value of α, the traveling speed may have such dependence on α. Qualitatively, this is due to the fact that the fluid not only carries heat downwards (small α region in Fig. 5), but also makes the temperature field uniform and thus suppresses the heat diffusion (large α region in Fig. 5).

VI. CONCLUSIONS

We have shown that an icicle covered with a thin layer of water flow makes wavelike undulations on the ice during solidification and that the preferred wavelength is determined by a MS-like theory. Thermal diffusion in air makes the wavelength shorter, i.e., the amplification factor becomes larger for shorter wavelengths. On the other hand, thermal diffusion in a thin layer of water flow makes the wavelength larger, i.e., the amplification factor becomes smaller for shorter wavelengths. From these two effects, a specific wavelength emerges with a maximum amplification factor of fluctuation. The thermal diffusion in the thin layer of water flow works just like the Gibbs-Thomson effect because the water flow makes the temperature distribution more uniform and thus inhibits the Laplace instability. This is one of our main results.

Our λ_{max} depends on θ and flow quantity $Q\equiv2\pi Rh_0\overline{U}=lh_0\overline{U}$. ($\theta$ dependence was observed for flow in an inclined gutter experiment: Fig. 2. For an icicle, $\theta=\pi/2$ should be used.)

$$\lambda_{\text{max}}=\frac{1}{D\alpha_{max}}\left(\frac{\nu}{g\pi\sin\theta}\right)^{1/3}\left(\frac{3Q}{2R}\right)^{4/3},\tag{82}$$

where we have used the relative Nusselt equation [8],

$$h_0=\left[\frac{\nu Q}{g\pi R\sin\theta}\right]^{1/3}.\tag{83}$$

The θ dependence of the wavelength for the ramp case is given by Matsuda [2] experimentally as

$$\lambda \sim \frac{8.2}{\sin^{\gamma}\theta}\ (\mathrm{mm}), \tag{84}$$

with $\gamma = 0.6 \sim 1$. However, the number of data for plotting is few, and thus we cannot get a definite result experimentally. γ is 0.3 in our theory. A difference exists, but it is not a large disagreement qualitatively.

In nature, all icicles have their own flow rates Q, but almost all have ripples with the same wavelength. This is explained by our analysis because the wavelength depends on the ratio of Q to R, not only on Q itself. It is then natural to assume that Q is proportional to R in nature. The selected wavelength of our analysis does not depend explicitly on external temperature. Although the mean growth rate V and also the amplification factor increase with decrease in temperature, the selected wavelength with the maximum amplification factor is independent of icicle growth rate (77).

We have also shown that surface ripples are expected to travel downwards during icicle growth with a speed of 0.5 times the average normal growth rate of the ice. This should be checked by experiments. Our theory can be used to map the waves around mineral stalagmite by changing the diffusion equation from temperature field to a solute density field. Furthermore, our diffusion equation in the fluid is mathematically similar to the Schrödinger equation for a harmonic oscillator having a complex valued potential. Therefore, it may be possible to use the algebraic method for analysis. This issue will be discussed elsewhere.

ACKNOWLEDGMENTS

The authors are grateful to Professor R. Takaki and Dr. P.L. Olivier for the valuable discussions. One of the authors, N.O., thanks Professor K. Fujii for his continuous encouragement. The authors would like to thank Professor E. Yokoyama, Dr. Nishimura, and Professor R. Kobayashi for the helpful discussions and encouragement and K. Norisue for her help.

APPENDIX

We define the fluctuation fields $\tilde{\psi}$ and $\tilde{P}$ by the following relation:

$$\psi = -\tfrac{1}{3}y^3 + y^2 + \tilde{\psi}(x,y), \tag{A1}$$

$$P = (1-y)\cot\theta + \hat{P} + \tilde{P}. \tag{A2}$$

Then for the fluctuation fields, we have the following equations:

$$\tilde{\psi}_{yyyy} = \mu\,\mathrm{Re}[(-y^2+2y+\tilde{\psi}_y)\tilde{\psi}_{xyy} - (-2+\tilde{\psi}_{yyy})\tilde{\psi}_x], \tag{A3}$$

$$\tilde{P}_x = \frac{1}{2\mu}\tilde{\psi}_{yyy} - \frac{\mathrm{Re}}{2}[(-y^2+2y+\tilde{\psi}_y)\tilde{\psi}_{xy} - (-2y+2+\tilde{\psi}_{yy})\tilde{\psi}_x], \tag{A4}$$

$$\tilde{P}_y = 0. \tag{A5}$$

The boundary conditions are

$$\tilde{\psi}_{x\,SL} = 0, \tag{A6}$$

$$\tilde{\psi}_{y\,SL} = \eta^2 \sin^2 x - 2\eta\sin x, \tag{A7}$$

$$\tilde{P}_{AL} = -\frac{W_0}{\sin\theta}(\tilde{h}_{xx} - \eta\sin x) + (\tilde{h} + \eta\sin x)\cot\theta, \tag{A8}$$

$$\tilde{\psi}_{yy\,AL} = 2(\tilde{h} + \eta\sin x), \tag{A9}$$

$$\tilde{\psi}_{x\,AL} = (\tilde{h}_x + \eta\cos x)[(1+\eta\sin x + \tilde{h})^2 - 2(1+\eta\sin x+\tilde{h}) - \tilde{\psi}_{y\,AL}], \tag{A10}$$

where the AL surface is determined by $y = 1 + \eta\sin x + \tilde{h}$, and the SL surface is determined by $y = \eta\sin x$.

To solve the above equations, we assume the solutions have the form

$$\tilde{\psi} = \tilde{\psi}^{(0)} + \mu\tilde{\psi}^{(1)} + \cdots, \tag{A11}$$

$$\tilde{P} = \tilde{P}^{(0)} + \cdots, \tag{A12}$$

$$\tilde{\psi}^{(0)}_{yyy} = 0, \tag{A13}$$

and we neglect higher orders in μ. The solutions for the zeroth-ordered stream function and pressure are

$$\tilde{\psi}^{(0)} = (\tilde{h} + \eta\sin x)y^2 - [\eta^2\sin^2 x + 2(1+\tilde{h})\eta\sin x]y + \left[(1+\tilde{h})\eta^2\sin^2 x + \frac{1}{3}\eta^3\sin^3 x\right], \tag{A14}$$

$$\tilde{P}^{(0)} = -\frac{W_0}{\sin\theta}(\tilde{h}_{xx} - \eta\sin x) + (\tilde{h}+\eta\sin x)\cot\theta. \tag{A15}$$

To obtain the first-order stream function, we put the above solution into the following equation:

$$\tilde{\psi}^{(1)}_{yyy} = -\frac{2W_0}{\sin\theta}(\tilde{h}_{xxx} - \eta\cos x) + 2(\tilde{h}_x + \eta\cos x)\cot\theta + \mathrm{Re} \times [(-y^2+2y+\tilde{\psi}^{(0)}_y)\tilde{\psi}^{(0)}_{xy} - (-2y+2+\tilde{\psi}^{(0)}_{yy})\tilde{\psi}^{(0)}_x], \tag{A16}$$

which is obtained by Eq. (A4) with the help of Eq. (A15). This expression is consistent with Eq. (A3). After some integrations with the boundary conditions, we obtain

$$\tilde{\psi}^{(1)}=\frac{\mathrm{Re}}{30}(1+\tilde{h})\tilde{h}_x\ y^5-\frac{\mathrm{Re}}{6}\eta(1+\tilde{h})\tilde{h}_x\sin xy^4+\frac{\mathrm{Re}}{3}\eta^2\times(1+\tilde{h})\tilde{h}_x\sin^2 xy^3+\frac{1}{3}\left[-\frac{W_0}{\sin\theta}(\tilde{h}_{xxx}-\eta\cos x)+(\tilde{h}_x+\eta\cos x)\cot\theta\right]y^3+\frac{1}{2}C_1(x)y^2+C_2(x)y+C_3(x). \quad (A17)$$

C_1, C_2, C_3 are determined by the boundary conditions. The results are

$$C_1=-2(1+\tilde{h}+\eta\sin x)\left[\mathrm{Re}(1+\tilde{h})\tilde{h}_x\left\{\frac{1}{3}(1+\tilde{h}+\eta\sin x)^2-(1+\tilde{h})\eta\sin x\right\}-\frac{W_0}{\sin\theta}(\tilde{h}_{xxx}-\eta\cos x)+(\tilde{h}_x+\eta\cos x)\cot\theta\right], \quad (A18)$$

$$C_2=-\frac{1}{2}\mathrm{Re}(1+\tilde{h})\tilde{h}_x\eta^4\sin^4 x+\left[\frac{W_0}{\sin\theta}(\tilde{h}_{xxx}-\eta\cos x)-(\tilde{h}_x+\eta\cos x)\cot\theta\right]\eta^2\sin^2 x-C_1(x)\eta\sin x, \quad (A19)$$

$$\frac{\partial C_3}{\partial x}=-\frac{\mathrm{Re}}{5}[(1+\tilde{h})\tilde{h}_x]_x\eta^5\sin^5 x-\frac{\mathrm{Re}}{2}(1+\tilde{h})\times\tilde{h}_x\eta^5\sin^4 x\cos x+\frac{\eta^3}{3}\left[\frac{W_0}{\sin\theta}(\tilde{h}_{xxxx}+\eta\sin x)-(\tilde{h}_{xx}-\eta\sin x)\cot\theta\right]\sin^3 x-\frac{\eta^2}{2}\partial_x C_1(x)\sin^2 x-\eta\partial_x C_2(x)\sin x. \quad (A20)$$

Now we put $\tilde{\psi}=\tilde{\psi}^{(0)}+\mu\tilde{\psi}^{(1)}$ into Eq. (A10). We now have

$$2(1+\tilde{h})^2\tilde{h}_x+\mu[\tilde{\psi}_x^{(1)}{}_{AL}+(\tilde{h}_x+\eta\cos x)\tilde{\psi}_y^{(1)}{}_{AL}]=0. \quad (A21)$$

We expand the fluctuation of water-layer thickness as

$$\tilde{h}=\tilde{h}^{(0)}+\mu\tilde{h}^{(1)}, \quad (A22)$$

and by putting it into the above equation, we have $\tilde{h}_x^{(0)}=0$, and so we can use

$$\tilde{h}^{(0)}=0. \quad (A23)$$

This can be done by redefining h_0 after subtracting a constant. Then $\tilde{h}^{(1)}$ is determined by

$$\tilde{h}_x^{(1)}=-\tfrac{1}{2}[\tilde{\psi}_x^{(1)}{}_{AL}+\eta\cos x\,\tilde{\psi}_y^{(1)}{}_{AL}]_{\tilde{h}=0}. \quad (A24)$$

From the fact that $\tilde{h}$ starts from $O(\mu)$ in its expansion, we can determine $\tilde{\psi}^{(1)}$ as

$$\tilde{\psi}^{(1)}=\left(\frac{W_0}{\sin\theta}+\cot\theta\right)[\tfrac{1}{3}\eta\cos xy^3-\eta\cos x(1+\eta\sin x)y^2+\{\eta^3\sin^2 x\cos x+2\eta^2\sin x\cos x\}y]+C_3, \quad (A25)$$

$$\partial_x C_3=\eta^3\sin x\left(\frac{W_0}{\sin\theta}+\cot\theta\right)[\tfrac{4}{3}\eta\sin^3 x-\eta\sin x+3\sin^2 x-2]. \quad (A26)$$

From the above expression and Eq. (A24), we obtain the following simple relation:

$$\tilde{h}_x^{(1)}=-\frac{\eta}{3}\left(\frac{W_0}{\sin\theta}+\cot\theta\right)\sin x. \quad (A27)$$

Furthermore,

$$\tilde{h}^{(1)}=\frac{\eta}{3}\left(\frac{W_0}{\sin\theta}+\cot\theta\right)\cos x. \quad (A28)$$

The height of the AL surface is

$$\xi(x)=1+\eta\sin x, \quad (A29)$$

whereas the stream function is

$$\psi=-\tfrac{1}{3}y^3+y^2+\tilde{\psi}^{(0)}(\tilde{h})+\mu\tilde{\psi}^{(1)}=-\tfrac{1}{3}(y-\eta\sin x)^3+(y-\eta\sin x)^2. \quad (A30)$$

[1] T. Tozuka, Denki Kagaku **8**, 218 (1938) (in Japanese); C. Knight, J. Cryst. Growth **49**, 193 (1980); N. Maeno and T. Takahashi, Low Temp. Sci. **43**, 125 (1984); **43**, 139 (1984); L. Makkonen, J. Glaciol. **34**, 116 (1988); K. Szilder and E.P. Lozowski, Ann. Glaciol. **19**, 141 (1994); N. Maeno, L. Makkonen, K. Nishimura, K. Kosugi, and T. Takahashi, J. Glaciol. **40**, 319 (1994).
[2] S. Matsuda, Master's thesis, Institute of Low Temperature Science, Hokkaido University, 1997 (in Japanese).
[3] W.W. Mullins and R.F. Sekerka, J. Appl. Phys. **35**, 444 (1964); see also Tamas Vicsek, *Fractal Growth Phenomena* (World Scientific, Singapore, 1989); for the theory of Crystal Growth, general textbooks are, for example, Ivan V. Markov, *Crystal Growth for Beginners* (World Scientific, Singapore, 1995); A. A. Chernov, *Modern Crystallography* III, Springer Series in Solid-State Sciences 36 (Springer, Berlin, 1984).
[4] S.R. Coriell and Robert L. Parker, J. Appl. Phys. **36**, 632 (1965); S.R. Coriell and S.C. Hardy, *ibid.* **40**, (1969); S.C. Hardy and S.R. Coriell, J. Cryst. Growth **3**, 569 (1968); Y. Furukawa and K. Nagashima, Appl. Math. Sci. **7**, 28 (1997) (in

Japanese), and related references are therein.

[5] J.S. Wettlaufer, M.G. Worster, L. Wilen, and J.G. Dash, Phys. Rev. Lett. **76**, 3602 (1996).

[6] G.D. Ashton (unpublished); G.D. Ashton and J.F. Kennedy, J. Hydraul. Div., Am. Soc. Civ. Eng. **98**, 1603 (1972); K.L. Carey, Geol. Surv. Prof. Pap. **550-B**, B192 (1966); R.R. Gilpin, T. Hirata, and K.C. Cheng, J. Fluid Mech. **99**, 619 (1980); K.S. Hsu, Ph.D. thesis, University of Iowa, 1973, p. 147; K.S. Hsu, F.A. Locher, and J.F. Kennedy, J. Heat Transfer **101**, 598 (1979); P.A. Larsen, J. Boston Soc. Civ. Eng. **56**, 45 (1969); C.B. Thorsness and T.J. Hanratty, AIChE J. **25**, 686 (1979); summary is given in M. Epstein and F.B. Cheung, Annu. Rev. Fluid Mech. **15**, 293 (1983).

[7] D.J. Benney, J. Math. Phys. **45**, 150 (1966).

[8] L. Landau and E. Lifschitz, *Fluid Mechanics*, 2nd ed. (Pergamon, Oxford, UK, 1987).

[9] The amplification rate of a wave (fluctuation) depends on its wavelength. Only the wave with the largest amplification rate can survive during the development of the fluctuations, and other modes will be observed as lower-amplitude noise. The constant rate of $\dot{\delta}/\delta$ means that the growth is exponential in time; hence, small differences in this constant result in large differences in the fluctuation amplitude at long times. In this sense, a mode distribution like that in Fig. 4 will be hidden in the external noise and thus not observed in experiments. This situation is the same as that in the original MS theory.